Computational modeling of the secondary rod pathway contribution to the retinal output

Laetitia Raison-Aubry, Loïs Naudin, Nange Jin, Christophe Ribelayga, Laure Buhry

Computational modeling of the secondary rod pathway contribution to the retinal output

Laetitia Raison-Aubry*
Université de Lorraine
CNRS
LORIA
Nancy, France
laetitia.raison-aubry@loria.fr

Loïs Naudin*
Université de Lorraine
CNRS
LORIA
Nancy, France
lois.naudin@gmail.com

Nange Jin
Department of Vision Sciences
College of Optometry
University of Houston
Houston, TX, USA
njin@central.uh.edu

Christophe Ribelayga
Department of Vision Sciences
College of Optometry
University of Houston
Houston, TX, USA
cpribela@central.uh.edu

Laure Buhry
Université de Lorraine
CNRS
LORIA
Nancy, France
laure.buhry@loria.fr

***Abstract*—In the retina, signals originating from rod and cone photoreceptors can reach retinal ganglion cells (RGCs) through different pathways. The secondary rod pathway is functionally important under mesopic light, such as at dawn or dusk. Electrical synapses (gap junctions) between rods and cones form the entry to the secondary rod pathway. Recent experimental observations indicate that these gap junctions are plastic, changing with the time of day and/or light/dark adaptation. However, the impact of this plasticity on the contribution of the secondary rod pathway to RGC activity remains elusive. As a first step, we model the spatial topology and connectivity of the secondary rod pathway of the mouse retina and test the light responses of OFF RGCs to dim light stimuli. Our results corroborate previously published electrical recordings thereby establishing the validity of the model and its suitability to further study rod/cone coupling plasticity.**

I. Introduction

The retina is a sensory organ located in the back of the eye and whose role is to detect light stimuli and process early visual information. Light is captured by photoreceptors (rods and cones), and converted into electrical potentials through the process of phototransduction. Electrical signals originating from photoreceptors are conveyed through secondary neurons (horizontal, bipolar and amacrine cells) to retinal ganglion cells (RGCs) – the output neurons of the retina whose axons project to higher processing centers in the brain. At the circuit level, rod and cone signals can travel across the retina through several distinct pathways: three different rod pathways and the cone pathway. Recent efforts have been made to experimentally characterize the secondary rod pathway [1]. Yet, accumulating evidence that the entry of the secondary rod pathway – the rod/cone gap junction – shows a high degree of plasticity [2] warrants further investigation of the contribution of this rod pathway to RGC activity.

To gain biological insight into the contribution of the secondary rod pathway and the impact of rod/cone gap junction plasticity to the retinal output, computational modeling could be a valuable asset. In that sense, our paper aims at developing a detailed model of the secondary rod pathway in the mouse retina with the goal to reproduce experimental data to validate the model. Here, we use a bottom-up approach consisting in connecting single cells into circuits and circuits into systems. Each cell of the secondary rod pathway is modeled using a single-point conductance-based model (CBM). In addition, and contrarily to previous studies [3]–[5], our model is based on a realistic representation of the spatial topology and connectivity of the mouse retina. Finally, we show that our detailed model is able to qualitatively reproduce the output of the secondary rod pathway – the behavior of RGCs – in response to a series of dim light stimuli. This shows the suitability of our model to further study rod/cone coupling plasticity that will be implemented in future works.

The remainder of the paper is organized as follows. Section II presents the spatial topology and connectivity of the secondary rod pathway in the mouse retina, as well as the model of each cell of the pathway and the photocurrent equation. Then, Section III shows the spatial topology and connectivity simulated from our modeling framework, and the simulated light responses of the RGC against the experimental ones. Finally, Section IV discusses the potential implications of our modeling workflow.

II. Materials and Methods

In this section, we first present the connectivity map of the secondary rod pathway to the transient OFF alpha retinal ganglion cells (tOFF αRGCs). Then, we describe the models of each cell composing this pathway, as well as the synaptic model that governs the interactions between the different components of the pathway.

*co-first authors: these authors have equally contributed to this work.

A. Connectivity map of the secondary rod pathway

The secondary rod pathway is composed of the rods, cones, CBCs (Cone Bipolar Cells), and RGCs – the output of the pathway. We model the OFF component of this pathway to a single tOFF αRGC. Fig. 1 summarizes the convergence and divergence relationship between each cell population to a single tOFF αRGC based on anatomical knowledge from the mouse retina.

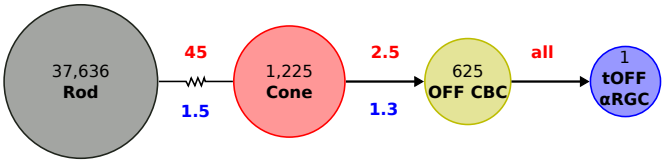

Fig. 1. Secondary rod pathway diagram. The numbers above each population denote their number of cells. The numbers in red denote the convergence and those in blue the divergence, between cell populations. "All" means that all OFF CBCs are connected to the tOFF αRGC.

In the photoreceptor network, rods outnumber cones by about 30:1 [6]. While rod/cone gap junctions are prevalent, there is little experimental support for rod/rod gap junctions, and cone/cone gap junctions are rare [7], [8], so we do not consider rod/rod and cone/cone connections in our model. Moreover, each cone makes gap junctions with around 45 nearby rods, while each rod contacts approximately 1.5 cones through gap junctions [7].

Also, the tOFF αRGC makes synaptic contacts with OFF CBC types 3A, 3B and 4 only [9], [10]. According to [10], each cone contacts approximately 1.3 CBCs of each type, and about 2.5 cones provide input to a single OFF CBC. Finally, we connect all OFF CBCs to the single tOFF αRGC.

To preserve the convergence and divergence ratio between each population of cells, we calculate their number according to the equation $N_{pre}/N_{post} = convergence/divergence$ where N_{pre} and N_{post} denotes the number of cells in the pre- and post-synaptic groups, respectively; and $convergence$ and $divergence$ denote the ratio of convergence and divergence between each cell group as described above. Following this methodology, we obtain a set of cells which comprises 37,636 rods, 1,225 cones, 625 OFF CBCs, and 1 tOFF αRGC, consistent with experimental data in the mouse retina [10].

B. Models

1) Photocurrent model: Both rods and cones respond to light but with different sensitivities. Rods can detect as few as a single photon whereas the cone threshold requires a few dozens [11]. This implies that we can omit the cone response under dim light conditions when individual rods receive one or a few photons on average. To model changes in the rod dark current caused by the dim light transduction process, we use a simulated photocurrent waveform, slightly adapted from [11], as input in the form $I_{photo} = I_{amp}[1 - \exp(-(t - b_1)/\tau_1) - \exp(-(t - b_2)/\tau_2]$ with I_{amp} the amplitude of the photocurrent (in pA), b_1 and b_2 the inflection points of the photocurrent trajectory, and τ_1 and τ_2 time constants (in ms). In this paper, we set $b_1 = 1000$, $b_2 = 1500$, $\tau_1 = 100$ and $\tau_2 = 100$.

2) Cell models: For each cell we use a single-point CBM that describes the evolution of the membrane potential V by a general equation of the form $C\mathrm{d}V/\mathrm{d}t = -\sum_{ion} I_{ion} + I$ where C is the membrane capacitance, $\sum_{ion} I_{ion}$ is the total current flowing accross the cell membrane, and I is an applied current. For the rod and cone cells, we use the CBM described in [12] and [13], respectively. For the OFF CBCs, we use the CBM reported in [4], and for the RGC the CBM described in [14]. Slight modifications have been made to the conductance values of these models in order to reproduce the qualitative shape of their steady-state current reported in the literature. Indeed, the steady-state current plays a paramount role in the dynamics of non-spiking neurons since it determines their qualitative features [15]. All the currents and the parameter values of each model are then reported in Table I.

TABLE I
BIOPHYSICAL MODEL PARAMETERS

	Rod	**Cone**	**CBC**	**RGC**
I_{Ca}	4 / 40	4.92 / 40	0.55 / 30	44 / 40
I_{Na}	–	–	–	1000 / 35
I_{Kv}	10 / −74	2 / −80	2 / −58	240 / −75
I_h	2.5 / −32	3.5 / −32.5	0.975 / −17.7	–
I_{KCa}	5 / −74	0.5 / −80	8.5 / −58	1 / −75
I_L	0.52 / −74	1 / −63	0.73 / −53	1 / −65
I_{Cl}	1.3 / −20	6.5 / −45	–	–
I_A	–	–	–	720 / −75

The first number denotes the maximal conductances (in nS), and the second number denotes the reversal potential (in mV).

3) Synaptic model: Several experimental studies have shown that the mode of neurotransmitter release in the retina is graded [16]. A 'graded synaptic connection' is one in which incremental changes in the membrane potential of the presynaptic neuron cause incremental changes in the membrane potential of the postsynaptic neuron [17]. To model this, we use the graded synaptic model described in [18], and adjust some parameters to reproduce the qualitative experimental behavior of the RGC described in [1].

4) Connectivity: We connect rods and cones with a probability that is modulated according to a 2-dimensional Gaussian of the distance between the cells, so that convergence and divergence between rods and cones are preserved. We proceed in the same way to connect cones to OFF CBCs. Finally, we connect all CBCs to a single tOFF αRGC.

III. RESULTS

In this section, we first implement the spatial connectivity of the secondary rod pathway, and we compare it with data from the literature. Then, we compare the behavior of our simulated tOFF αRGC with the experimental results of [1]. All this was done using the Brian2 simulation environment [19].

A. Generation of the retina network

In our model, the retinal cells are distributed in a 266 μm long square grid (*i.e.* $70,756$ μm^2), which is an accurate

representation of the experimental spatial topology of the mouse retina for a single tOFF αRGC. Indeed, tOFF αRGCs have large dendritic fields of about 300 μm diameter [20]. In other words, the set of presynaptic cells to a tOFF αRGC - including the photoreceptor network and the OFF CBCs in the case of the secondary rod pathway - thus extends over an area of about $70,685\ \mu m^2$. Within this area, the cells are evenly and equidistantly distributed (Fig. 2.A), with a rod/rod distance of approximately 1.37 μm, a cone/cone distance around 7.6 μm, and a OFF CBC/OFF CBC distance of approximately 10.64 μm, which is also consistent with biological observations [9], [10].

In addition, our model takes into account the spatial connectivity in the secondary rod pathway in the mouse retina. In particular, the average number of connections per cell is maintained (e.g., in our model the divergence and convergence from rods to cones is, respectively, 1.56 and 47 on average, as illustrated in Fig. 2.B).

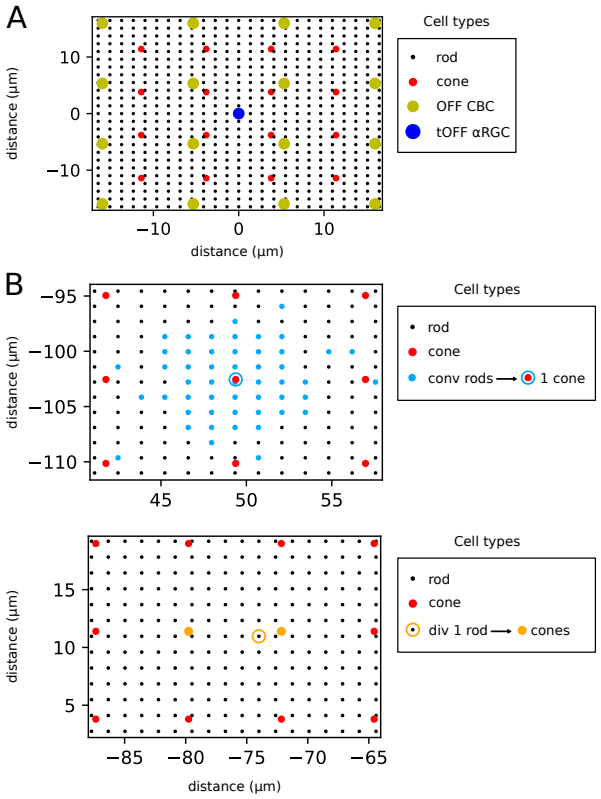

Fig. 2. **(A)** Topology of the secondary rod pathway (portion of the modeled retinal cell grid centered on the tOFF αRGC). **(B)** Connectivity in the photoreceptor network. (Top) Convergence: all presynaptic rod contacts for one randomly-chosen cone. (Bottom) Divergence: all postsynaptic cone contacts for one randomly-chosen rod.

B. Comparison with the experimental behavior of RGCs

Here we simulate the secondary rod pathway, made up of about 40,000 cells, following the experimental stimulation protocol described in [1]. This protocol consists of a 1-s period of darkness, followed by a dim light stimulus of 500-ms in duration, and a second period of darkness of 2.5 seconds. The simulation time using Brian2 is about 3 minutes on a regular laptop 11th Gen Intel® Core™ i5-1135G7 @ 2.40GHz × 8, which is a very short simulation time given the model complexity.

Fig. 3A shows the simulated and experimental responses of a tOFF αRGC in response to three different light stimulus intensities delivering 0.06, 2, and 20 effective isomerizations R*/rod/sec. It can be observed that our model reproduces the qualitative features of the experimental ones [1]. Indeed, at the weakest intensities, when only 1 rod out of 17 receives a single photon (2 pA), the tOFF αRGC does not elicit a noticeable response. At the brightest intensity, when each rod absorbs 20 photons (10 pA), the cell stops firing for most of the time the light stimulus is present. At the intermediate intensity, when each rod absorbs 2 photons (4 pA), a small yet significant decrease in firing occurs. Furthermore, the frequency of the spikes of our simulated tOFF αRGC is approximately 85 Hz, which is close to the experimental value [1].

Regarding the threshold of the secondary rod pathway, defined as the stimulus intensity to generate 5% of maximal response to the light stimulus, studies have shown that it is around 2 photons/rod/sec [1]. This approximately corresponds to a rod photocurrent of 4 pA. Similarly, the response threshold of our simulated tOFF αRGC is around 3.92 pA (Fig. 3B).

In addition, because there is no noise nor heterogenity in our model, the light response of our simulated tOFF αRGC, once its threshold is reached, is binary, in contrast with the experimental traces (Fig. 3A). This also explains the slight discrepancies in the spike firing times between the experimental and our simulated cell. Furthermore, the model does not capture the experimental overshoot in the tOFF αRGC - i.e. spikes arise before the photocurrent drops back to 0 pA. This phenomenon – known as "rebound excitation" – is partly due to the intrinsic properties of RGCs, in particular the biophysical properties of the I_h and I_{Ca} currents [21]. These currents, together with continuous noise in the circuit and mechanisms of feedback and/or inhibition will be implemented to improve the realism of the model.

IV. Discussion and Conclusion

In this paper, we model the spatial topology and connectivity of the secondary rod pathway of the mouse retina and test the light responses of tOFF αRGCs to dim light stimuli. We are able to reproduce the light responses of a RGC with a behavior similar to what has been experimentally reported [1]. In particular, the secondary rod pathway of the mouse retina has a threshold around 2 photons/rod/sec [1], corresponding to a photocurrent amplitude of 4 pA. The model sets the threshold around 3.92 pA (Fig. 3B).

Although the model effectively replicates the essential qualitative features of the experimental data from the secondary rod pathway, it could nevertheless be improved by addressing some limitations. First, as previously highlighted, our model lacks both noise and overshoot of the tOFF αRGC response that we could take into account. Second, we will need to add the other rod pathways, namely the primary and the tertiary rod pathway. The circuit elements of these pathways have been well-characterized and their respective contributions to tOFF αRGCs have been recently established [1], [20]. Modeling the respective contributions of all 3 rod pathways and cone pathway to a single RGC will further validate our model.

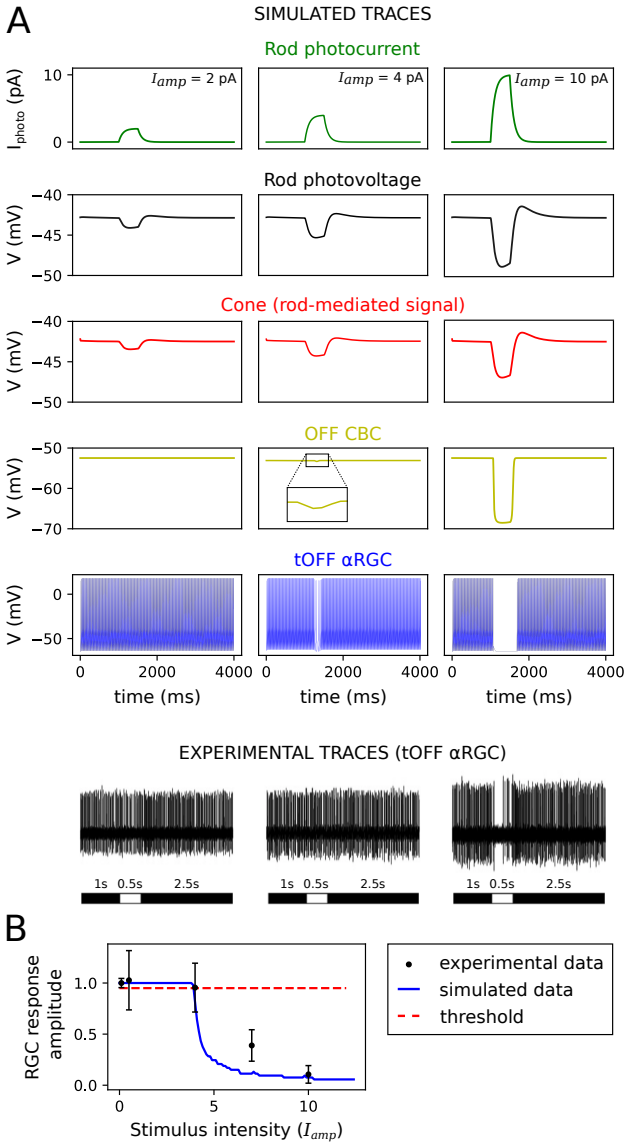

Fig. 3. **(A)** Comparison of the simulated RGC behavior with the experimental one for three different intensities of photocurrent (0.06, 2, and 20 R*/rod/s). For the lowest intensity, only 1/17 rod receives the photocurrent. The experimental data are reproduced from [1] with permission. **(B)** Normalized spiking frequency of the tOFF αRGC during lights-on for increasing photocurrent amplitudes. The threshold of the secondary rod pathway (red) is defined as the stimulus intensity to generate 5% of maximal response to the light stimulus [1]. Experimental data are means $\pm$ SEM (n = 5 cells).

Once these limitations are addressed, our model will be useful to study the functional importance of the plasticity of the rod/cone gap junction. Indeed, these coupling changes with the time of day and light/dark environmental conditions [2]. As the dynamic range of rod/cone spans over more than 1,000 pS [8], it is expected to dramatically affect the contribution of the secondary rod pathway to the retinal output. Because the pharmacological approach is limited (modulating rod/cone gap junctions will affect other gap junctions elsewhere in retinal circuits), our model will provide valuable insights into the functional impact of the modulation of rod/cone coupling.

ACKNOWLEDGMENT

We thank the INS2I-CNRS and LORIA for their financial support on the ModERN-Psy project. The authors thank also LUE for funding L.R.-A. travel grant. Research in the Ribelayga lab is supported by NIH grants R01EY029408, R01EY032508, RF1MH127343, and P30EY007551, and an Endowed Professorship from the FERV.

REFERENCES

[1] N. Jin, L.-M. Tian, I. Fahrenfort, Z. Zhang, F. Postma, D. L. Paul, S. C. Massey, and C. P. Ribelayga, "Genetic elimination of rod/cone coupling reveals the contribution of the secondary rod pathway to the retinal output," *Science Advances*, vol. 8, no. 13.

[2] C. Ribelayga and J. O'Brien, "Circadian and light-adaptive control of electrical synaptic plasticity in the vertebrate retina," in *Network Functions and Plasticity*.

[3] E. Iseri, P. Kosta, J. Paknahad, J.-M. C. Bouteiller, and G. Lazzi, "A computational model simulates light-evoked responses in the retinal cone pathway," in *2021 43rd IEEE EMBC Conference*.

[4] R. Publio, R. F. Oliveira, and A. C. Roque, "A computational study on the role of gap junctions and rod i h conductance in the enhancement of the dynamic range of the retina," *PLoS One*, vol. 4, no. 9, 2009.

[5] Y. Kamiyama, S. M. Wu, and S. Usui, "Simulation analysis of bandpass filtering properties of a rod photoreceptor network," *Vision research*, vol. 49, no. 9.

[6] L. D. Carter-Dawson and M. M. Lavail, "Rods and cones in the mouse retina. i. structural analysis using light and electron microscopy," *Journal of Comparative Neurology*, vol. 188, no. 2.

[7] N. Jin, Z. Zhang, J. Keung, S. B. Youn, M. Ishibashi, L.-M. Tian, D. W. Marshak, E. Solessio, Y. Umino, I. Fahrenfort, *et al.*, "Molecular and functional architecture of the mouse photoreceptor network," *Science advances*, vol. 6, no. 28.

[8] M. Ishibashi, J. Keung, C. W. Morgans, S. A. Aicher, J. R. Carroll, J. H. Singer, L. Jia, W. Li, I. Fahrenfort, C. P. Ribelayga, *et al.*, "Analysis of rod/cone gap junctions from the reconstruction of mouse photoreceptor terminals," *Elife*, vol. 11.

[9] M. Helmstaedter, K. L. Briggman, S. C. Turaga, V. Jain, H. S. Seung, and W. Denk, "Connectomic reconstruction of the inner plexiform layer in the mouse retina," *Nature*, vol. 500, no. 7461.

[10] C. Behrens, T. Schubert, S. Haverkamp, T. Euler, and P. Berens, "Connectivity map of bipolar cells and photoreceptors in the mouse retina," *Elife*, vol. 5.

[11] N. G. Jin, A. Z. Chuang, P. J. Masson, and C. P. Ribelayga, "Rod electrical coupling is controlled by a circadian clock and dopamine in mouse retina," *The Journal of physiology*, vol. 593, no. 7.

[12] D. E. Kourennyi, X.-d. Liu, J. Hart, F. Mahmud, W. H. Baldridge, and S. Barnes, "Reciprocal modulation of calcium dynamics at rod and cone photoreceptor synapses by nitric oxide," *Journal of neurophysiology*, vol. 92, no. 1.

[13] X.-D. Liu and D. E. Kourennyi, "Effects of tetraethylammonium on kx channels and simulated light response in rod photoreceptorss," *Annals of biomedical engineering*, vol. 32, no. 10.

[14] J. Fohlmeister, P. Coleman, and R. F. Miller, "Modeling the repetitive firing of retinal ganglion cells," *Brain research*, vol. 510, no. 2.

[15] L. Naudin, J. L. Jiménez Laredo, Q. Liu, and N. Corson, "Systematic generation of biophysically detailed models with generalization capability for non-spiking neurons," *PloS one*, vol. 17, no. 5.

[16] J. E. Dowling, *The retina: an approachable part of the brain*. Harvard University Press, 1987.

[17] A. Roberts and B. M. Bush, *Neurones without impulses: their significance for vertebrate and invertebrate nervous systems*, vol. 6. Cambridge University Press, 1981.

[18] B. Mulloney, "During fictive locomotion, graded synaptic currents drive bursts of impulses in swimmeret motor neurons," *Journal of Neuroscience*, vol. 23, no. 13.

[19] M. Stimberg, R. Brette, and D. F. Goodman, "Brian 2, an intuitive and efficient neural simulator," *Elife*, vol. 8.

[20] B. Krieger, M. Qiao, D. L. Rousso, J. R. Sanes, and M. Meister, "Four alpha ganglion cell types in mouse retina: Function, structure, and molecular signatures," *PloS one*, vol. 12, no. 7.

[21] P. Mitra and R. F. Miller, "Mechanism underlying rebound excitation in retinal ganglion cells," *Visual neuroscience*, vol. 24, no. 5.